ATLAS NOTE

March 10, 2008

E/p check of the single hadron energy scale using pions from minimum bias

N. Davidson and E. Barberio
The University of Melbourne

Abstract

In this note we ...

1 Introduction

Minimum bias was studied to determine the possibility of using $\pi^{\pm}$s from these events to check the single hadron energy scale for CaloTopoClusters using tracks in the inner detector. The momentum range studied was 1-10GeV.

some more intro. to come.

2 Datasets used

A list of the datasets used is given in Table 1. Samples were reconstructed with Athena 12.0.6. Different sub-versions of Athena 12.0.6 were used, but no significant deviations were observed in the hadronic energy scale between them. csc11 datasets were used where available. As the minimum bias csc11 dataset had less statistics than its mc12 counterpart, the later was used for tracks of higher pt which occur less frequently ($p_T \geq$5GeV). Unless otherwise stated all tables and figures of range $p_T < 5GeV$ show results from the csc11 dataset, while all $p_T \geq 5GeV$ results are from the mc12 dataset.
Single particle events were privately produced when no offical dataset was available.

Need to put in some numbers for the simulated cross-section and trigger.

Event Type	Dataset Name	Number of Events
minimum bias	trig1_misal1_csc11_V1.005001.pythia_minbias.recon.ESD.v12000601	250,000
	trig1_misal1_mc12_V2.005001.pythia_minbias.recon.ESD.v12000605	3,000,000
single $\pi^{\pm}$s	trig1_misal1_mc12.007421.singlepart_singlepi_et1.recon.ESD.v12000604	70,000
	trig1_misal1_mc12.007151.singlepart_eta_Et2.recon.ESD.v12000604	20,000
	privately produced π^-s with p_T=2 GeV (12.0.6.5 used for full simulation)	20,000
	trig1_misal1_mc12.007152.singlepart_eta_Et5.recon.ESD.v12000604	20,000
	privately produced π^-s with p_T=5 GeV (12.0.6.5 used for full simulation)	20,000
	trig1_misal1_mc12.007422.singlepart_singlepi_et10.recon.ESD.v12000604	100,000

Table 1: List of datasets used for low energy E/p study

3 Trigger rates and event selection

4 Track momentum reach and resolution

The transverse momentum range for tracks in 50k minimum bias monte carlo events is shown in Figure 1(a). This is equivalent to approximately 1 μb^{-1} of data.

To eliminate fake tracks and ensure an accurate momentum measurement, only tracks passing the following quality selection were considered.

- At least one hit in the B Layer of the pixel detector.
- No more than one hole in the other pixel and SCT layers.
- $\chi^2/ndof < 1.5$

Approximately 76% of tracks passed these criteria. The p_T range for $\pi^{\pm}$s with quality tracks is given by the hashed curve in Figure 1(a). This shows that minimum bias events can provide a source of $\pi^{\pm}$s to check the hadronic energy scale from 400 MeV, the energy required to reach the calorimeter, up to the energy covered by hadronically decaying taus.

Some more to come about the track resolution.

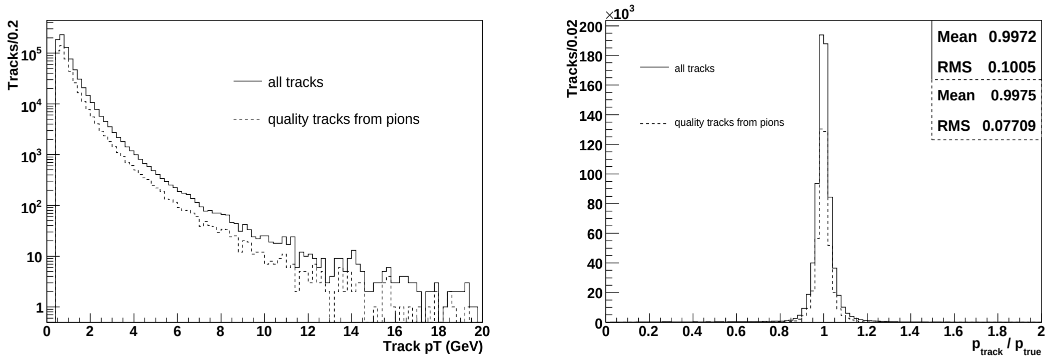

(a) p_T distribution

(b) p resolution

Figure 1: p_T distribution and p resolution for tracks from 50k csc11 minimum bias events

5 Energy of low p_T $\pi^{\pm}$s

The $\pi^{\pm}$ energy, E, in the calorimeter was found by extrapolating the track direction to the 2nd layer of the EM calorimeter using the TrackToCalo tool [**?**]. From this position a cone was defined, $\Delta R_{cone} = \sqrt{\Delta\phi^2 + \Delta\eta^2} = 1.0$ and the energy of each $\pi^{\pm}$ was calculated as the sum of all CaloTopoClusters within this cone. The background contribution from charged sources could not be eliminated in $|\eta| > 2.5$ with a track isolation cut due to the range of the inner detector. Because of this, CaloTopoClusters outside this range were not included in the $\pi^{\pm}$ energy sum. The $\pi^{\pm}$ tracks examined were limited to the range $|\eta| < 2.4$.

CaloTopoClusters [**?**] reconstructed with Athena 12.0.6 were, by default, calibrated to the hadronic scale with the local hadron calibration. This included some corrections for energy lost in dead material, but did not include corrections for energy lost in cells outside the cluster[1)]. The noise suppression factors of 4/2/0 meant a cluster was required to have a seed cell of absolute energy 4σ above electronic noise levels, the algorithm iteratively added neighboring cells while their absolute energy was 2σ above noise and in general all cells considered had to be above 0σ. For the very low energies examined, $p_T < 10$ GeV, many cells with true $\pi^{\pm}$ energy did not pass these conditions, resulting in an E/p well below 1. Therefore, in this study, biases to the E/p due to backgrounds could not be determined by the shift of the mean from 1. It was necessary to instead assess the background biases by comparing the distribution to a control $\pi^{\pm}$ sample known to be isolated from other particles. Hence, single particle events were examined to determine the expected distribution. Single $\pi^{\pm}$s of p_T = 1 GeV, 2 GeV, 5 GeV and 10 GeV, were compared respectively to $\pi^{\pm}$s in minimum bias of p_T=0.8-1.2 GeV, 1.6-2.4 GeV, 4-6 GeV, 8-12 GeV.

With real data the E/p performance will need to be check in bins of both energy and pseudorapidity, as the E/p distribution varied dramatically across $|\eta|$. However, due to limited statistics in the monte-carlo

[1)]From Athena 13 these corrections are included by default produced, binning in both η and p could not be done. Instead for this study we binned in p_T because minimum bias has a charged particle multiplicity relatively flat in η for a given p_T. Then we weighted tracks based on their position in $|\eta|$ so that the minimum bias and single particle control samples had the same $|\eta|$ distribution.

Figure 2 shows the E/p distribution for single $\pi^{\pm}$s with tracks in these p_T ranges. The peaks around 0 in the 1GeV and 2GeV cases are due to cell thresholds above noise not being meet and energy losses in upstream material.

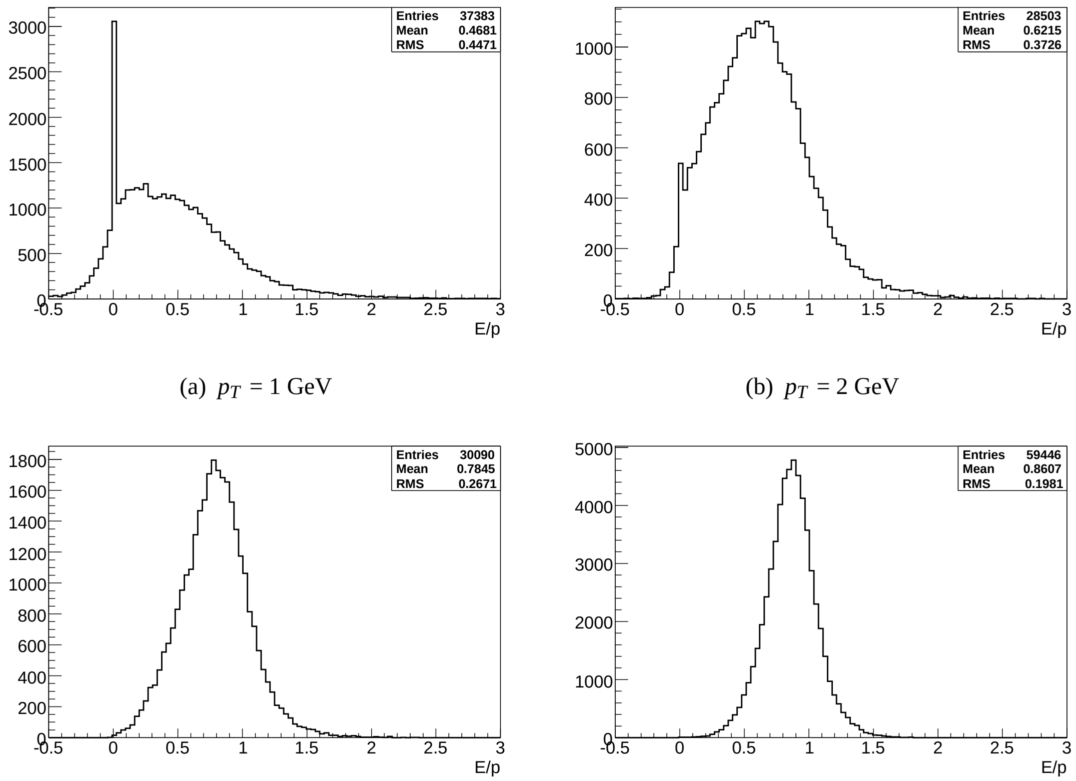

(a) p_T = 1 GeV

(b) p_T = 2 GeV

(c) p_T = 5 GeV

(d) p_T = 10 GeV

Figure 2: E/p distributions for ideal $\pi^{\pm}$s from single particle Monte Carlo. The samples used were uniform in $|\eta|$

6 Removal of extra particle contamination

In minimum bias, extra particles within the ΔR cone of the track considerably bias the measured $\pi^{\pm}$ energies. This is shown by the hashed curve in Figure 3.

The main source of background was found to be neutral particles, predominantly neutrons and photons (from π^0 decay). Charged particles also contributed to the background. The requirement of an isolated track was very effective in removing this contribution, however, it was limited by the range of the inner detector,$|\eta| < 2.5$, and the efficiency of track reconstruction, which can be as low as 80% for

$\pi^{\pm}$ at these energies [**?**].

Selection cuts were used to try to identify those $\pi^{\pm}$s that were isolated. This was not found to be sufficient to remove all the background and preserve the shape of the E/p distribution. Additionally, very few isolated $\pi^{\pm}$s with energy above 2 GeV were present in minimum bias. This is shown by the distance in ΔR between the $\pi^{\pm}$ track and additional particles in Figure 4. Therefore cuts were applied to reduce the overall contamination, as described next (Section 6.1), and an approach to estimate the remaining background energy (Section 6.2) and correct for it (Section 6.3) was studied. To assess this method, only tracks matched to a $\pi^{\pm}$ in the TrackTruthCollection were used. The effect from non-pion tracks is discussed in Section 7.

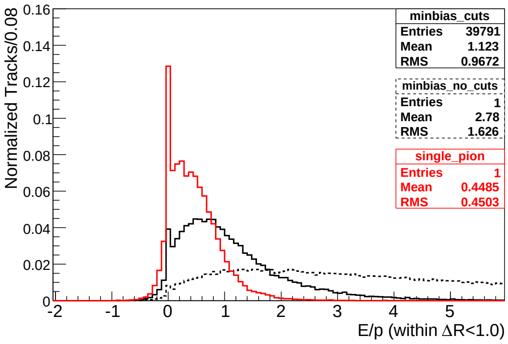

(a) p_T=1GeV

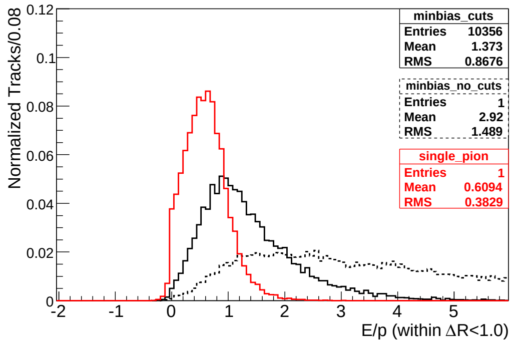

(b) p_T=2GeV

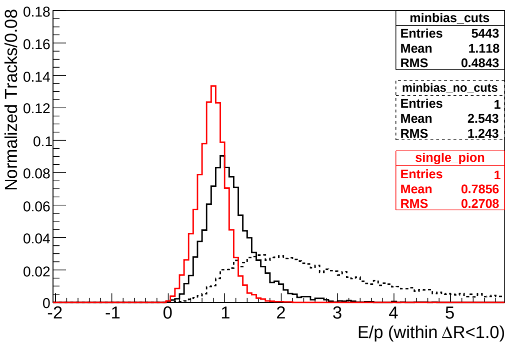

(c) p_T=5GeV

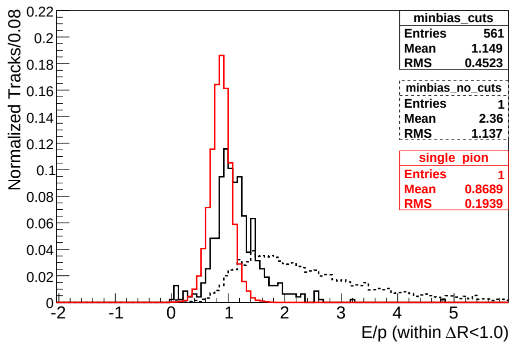

(d) p_T=10GeV

Figure 3: $\pi^{\pm}$ E/p distrubtions for minimum bias before and after cuts are applied (as described in 6.1) and single particles. The effect of applying the cuts is a large reduction in the contamination. However, some contamination is still visible when compared to the single particle distrubtions. For shape comparision the number of tracks was normalised to 1 in all three cases.

6.1 Contamination reduction with cuts

Three cuts were used to minimize the contamination from extra particles. The selection requirements differed slightly for $\pi^{\pm}$ with p_T >2GeV and $p_T \leq$2GeV due to fewer high p_T tracks in minimum bias and the different shower shapes. The efficiency of each cut is listed in Tables 2 and 3. This shows an overall reduction in the bias due to extra particle by approximately half. The bias to the E/p caused by

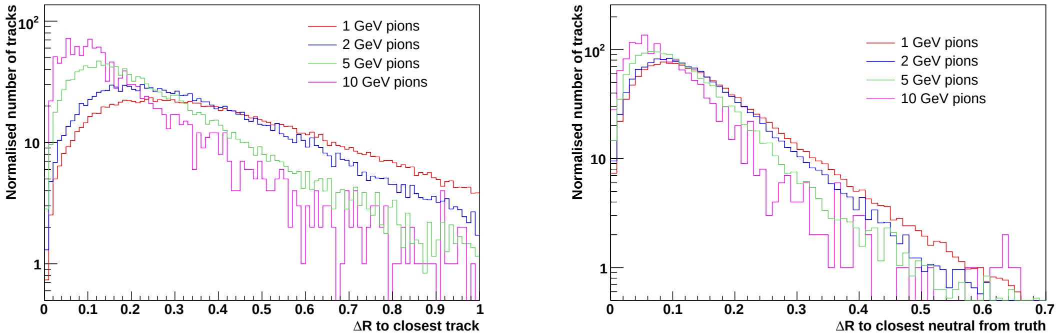

(a) ΔR to closest track after extrapolation to calorimeter (b) ΔR to closest stable neutral from truth information

Figure 4: Distribution of ΔR between pion track and closest other track (left) or closest neutral particle (right). The plots show that all pions in minimum bias are accompanied by another particle within $\Delta R < 1.0$.

applying the cuts can be estimated by the single particle sample. Here it is seen to be very small: 0.006 for 1GeV pions, 0.002 for 2GeV pions, 0.000 for 5GeV and 0.001 for 10GeV. This bias is primarily due to the isolation cut on energy in the hadronic calorimeter (3.). Cuts 1. and 2. are based on extra particles in the event, so should not bias the single pion sample and will only result in removing events with fake tracks.

Figure 3 shows the resulting E/p distribution before and after cuts, compared to single $\pi^{\pm}$s.

1. Tracks were isolated from other tracks by $\Delta R_{track\_isolation} > 0.4$. Where the track positions was taken at the 2nd layer of the EM calorimeter.
2. The $\pi^{\pm}$ track was required to be one of the harder tracks in the event.
    - $p_T / \sum_{all\_tracks} p_T > 0.1$ for p_T=1GeV, 2GeV.
    - $p_T / \sum_{all\_tracks} p_T > 0.3$ for p_T=5GeV, 10GeV.
3. The energy in the hadronic calorimeter was required to be small for CaloTopoClusters in the outer region $0.4 < \Delta R_{cone} < 1.0$ of the cone:
    - $< 0.01 \times p$ for p_T=1GeV, 2GeV.
    - $< 0.05 \times p$ for p_T=5GeV, 10GeV

6.2 Background measurement

The remaining bias due to the contamination within the ΔR cone was accounted for by measuring and deconvoluting the background. This is an approach similar to the one used in [1]. The method required classifying the cone surrounding the track into three region:

Cuts	1 GeV			2 GeV		
	Tracks per 250k events	**Minimum bias** $< E/p >$	**Single particle** $< E/p >$	**Tracks per 250k events**	**Minimum bias** $< E/p >$	**Single particle** $< E/p >$
Before cuts	579,300	2.786 ± 0.007	0.455 ± 0.002	137,300	2.920 ± 0.011	0.611 ± 0.002
1. Track Isolation	322,200	2.483 ± 0.008	0.455 ± 0.002	56,800	2.457 ± 0.015	0.611 ± 0.002
2. Event Track Energy	74,900	1.489 ± 0.011	0.455 ± 0.003	23,400	1.741 ± 0.016	0.611 ± 0.002
3. Isolation in H. Cal.	39,778	1.123 ± 0.005	0.449 ± 0.003	10,355	1.373 ± 0.009	0.609 ± 0.003

Table 2: Efficiency of cuts applied to p_T = 1GeV and 2GeV $\pi^{\pm}$. The mean was taken in the range $-2 < E/p < 6$ and all samples were weighted to have the same $|\eta|$ distribution.

Cuts	5 GeV			10 GeV		
	Tracks per 3mill. events	**Minimum bias** $< E/p >$	**Single particle** $< E/p >$	**Tracks per 3mill. events**	**Minimum bias** $< E/p >$	**Single particle** $< E/p >$
Before cuts	95,300	2.543 ± 0.011	0.786 ± 0.002	9,390	2.360 ± 0.014	0.868 ± 0.001
1. Track Isolation	25,000	1.760 ± 0.016	0.786 ± 0.002	1,430	1.410 ± 0.018	0.868 ± 0.001
2. Event Track Energy	7,500	1.206 ± 0.017	0.786 ± 0.002	722	1.199 ± 0.019	0.869 ± 0.001
3. Isolation in H. Cal.	5,443	1.118 ± 0.007	0.786 ± 0.002	561	1.149 ± 0.021	0.869 ± 0.001

Table 3: Efficiency of cuts applied to p_T = 5GeV and 10GeV $\pi^{\pm}$. The mean was taken in the range $-2 < E/p < 6$ and all samples were weighted to have the same $|\eta|$ distribution.

- A core region close to the track, where most of the $\pi^{\pm}$ energy was deposited, but very little background energy.
  - $\Delta R_{core} = 0.1$ for p_T=1 GeV or 2 GeV.
  - $\Delta R_{core} = 0.05$ for p_T=5 GeV and 10 GeV.
- A region in the electromagnetic calorimeter outside the core. EM_{outer_cone}, where most of the contaminating background energy was deposited.
- A region in the hadronic calorimeter outside the core where little background energy was deposited. HAD_{outer_cone}.

In general there was overlap between the $\pi^{\pm}$ and background energy outside the core, which made their separation impossible. However, late showering $\pi^{\pm}$s acting as mips through the electromagnetic calorimeter leave very little energy in EM_{outer_cone}. Hence, all energy measured in EM_{outer_cone} was from background sources. These late showering $\pi^{\pm}$s were used for measuring the contamination for all $\pi^{\pm}$s, as we assumed the $\pi^{\pm}$ penetrating depth was uncorrelated with the background[2)].

Late showering $\pi^{\pm}$s were identified by two selection criteria:

- The energy in the electromagnetic calorimeter within $\Delta R < 0.05$ of the track was less than $0.5 \times p$
- The energy in the hadronic calorimeter within $\Delta R < 0.05$ of the track was above $0.5 \times p$

The estimated background E/p distributions obtained in this way for EM_{outer_cone} are shown in Figure 5. Also shown is the energy for single $\pi^{\pm}$. This was used to indicate how much energy was deposited from the late showering $\pi^{\pm}$ in EM_{outer_cone}. As $\pi^{\pm}$ energy gets mistaken as background in this region, the mean E/p for single pions should be below 1% or the background energy will be overestimated. This results in an underestimate of final E/p after the background is subtracted. For 1 GeV $\pi^{\pm}$ (see Figure

[2)]This assumption may not hold as the proportion of out of cluster energy is reduced when showers overlap, as in the case of early showering $\pi^{\pm}$s with background particles. However it could not be checked in this study due to limited statistics.

5(a)) the pion energy in EM_{outer_cone} would cause an underestimate in the final E/p of approximately 0.02.

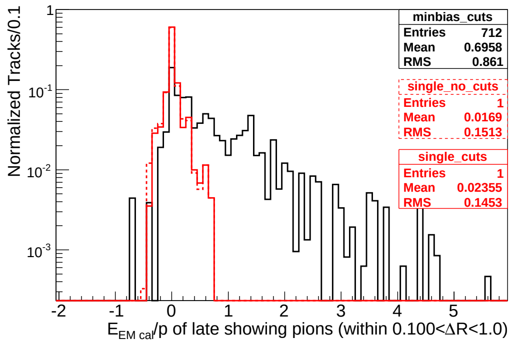

(a) p_T=1GeV

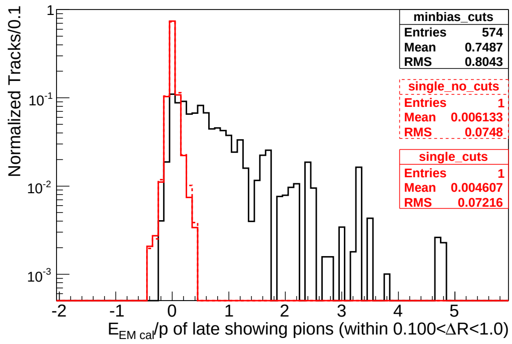

(b) p_T=2GeV

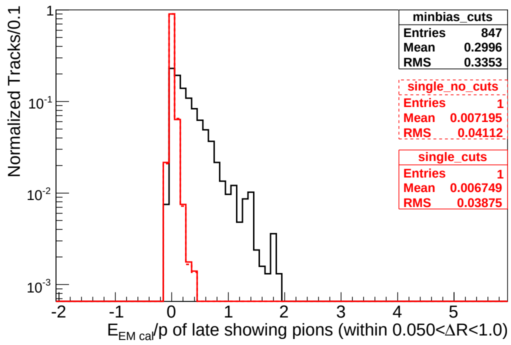

(c) p_T=5GeV

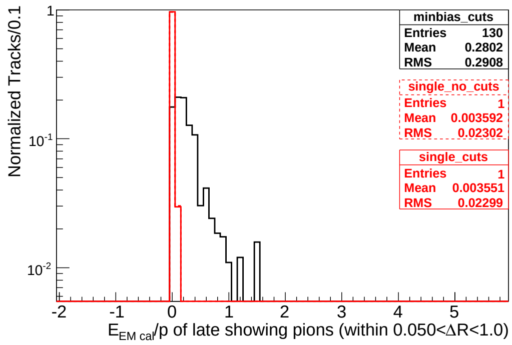

(d) p_T=10GeV

Figure 5: Distribution of E/p in EM_{outer_cone} for tracks associated with late showering pions in minimum bias and single $\pi^{\pm}$s samples

Another bias to the E/p can be caused by background in the other regions of the cone (HAD_{outer_cone} and the core) where contaminating energy can not be measured in situ. It can therefore not be corrected, so will need to be below %1. The contamination in these two region was checked by comparing the E/p for $\pi^{\pm}$s in minimum bias to single particles. The difference in the E/p mean is shown in Table 4 and was assumed to be due to contamination. As the combined contribution from HAD_{outer_cone} and the core can be as large as 0.03, the contamination would need to be reduced with further cuts if an E/p known to within 1% is to be obtained.

$\pi^{\pm}$ p_T	**Background in HAD_{outer_cone}**	**Background in core**	**Combined unmeasurable background**
1 GeV	0.012 ± 0.002	0.003 ± 0.003	0.015 ± 0.004
2 GeV	0.016 ± 0.002	0.010 ± 0.005	0.026 ± 0.005
5 GeV	0.012 ± 0.003	-0.002 ± 0.006	0.010 ± 0.007
10 GeV	0.020 ± 0.010	0.009 ± 0.018	0.029 ± 0.021

Table 4: $< E/p >$ of unmeasurable background. Calculated from the difference between $< E/p >$ for $\pi^{\pm}$s from minimum bias and single particle event in the listed cone region.

6.3 Correction for background

The E/p^{meas} distributions shown in Figure 3 are a convolution of the E/p distributions for isolated $\pi^{\pm}$s, E/p^{iso}, and the background contamination within the cone of the $\pi^{\pm}$. By deconvoluting the background from the measured E/p, we recovered E/p^{iso}.

The convolution can be written generally in term of the number of entries in a bin labelled *i* of the measured E/p histogram.

$$E/p_i^{meas} = \sum_j P_{ij} \times E/p_j^{iso}$$

where the elements of the matrix P_{ij} represent the probability of the contaminating background shifting the energy from bin j to bin i.

Each element of P_{ij} can be taken directly from the measured background histogram E/p^{contam}. This can be understood by considering the amount of contaminating energy required to shift the E/p from bin i to j. More specifically, if the bin at E/p=0 is labelled 0, then the energy contamination needed to shift the E/p from i to j can be found in bin i-j. This gives the migration matrix $P_{ij} = E/p_{(i-j)}^{contam}$. The probability of finding contamination with this energy, i-j, is given by the normalized background distribution. So that the diagonal of the matrix P_{ij} is the probability of no contamination and is taken directly from the peaks at 0 (see Figure 5). The $E/p_{(i-j)}^{contam}$ matrix is shown as a 2-d histogram for the case of 1GeV $\pi^{\pm}$s in Figure 6.

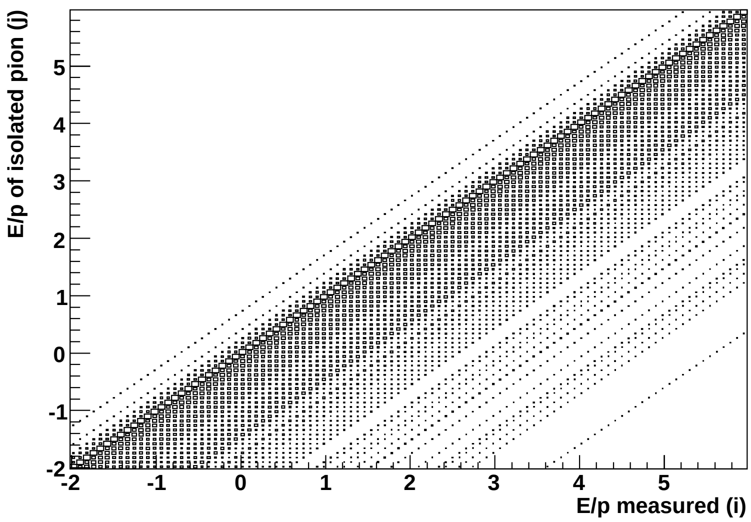

Figure 6: The migration matrix used for 1GeV $\pi^{\pm}$ in minimum bias. Entries are taken from the measured contaminating background in EM_{outer_cone}. The off-diagonal entries result in a positive bias to the isolated $\pi^{\pm}$ E/p.

The convolution can then be written as the set of *i* linear equations:

$$E/p_i^{meas} = \sum_j E/p_{(i-j)}^{contam} \times E/p_j^{iso}$$

The distribution E/p^{iso} can be extracted by solving this system via matrix inversion. However, the results are very sensitive to the statistical fluctuations of in both the migration matrix and measured E/p distribution.

To remove these fluctuations, the distributions were smoothed before solving the convolution equations. The background was fit with two exponential function, one above and one below zero. The measured E/p was fit with an exponential below zero, a 7th order polynomial above zero up to 1/2 the height maximum and an exponential function for the high E/p tail. The bin at E/p=0 and the two bins either-side of this bin were left unsmoothed. The result of these fits are shown in Figure 7 for 1GeV $\pi^{\pm}$s. The deconvoluted distributions obtained for E/p^{iso} are shown in Figure 8.

More to come on the unfolded distribution...including errors?

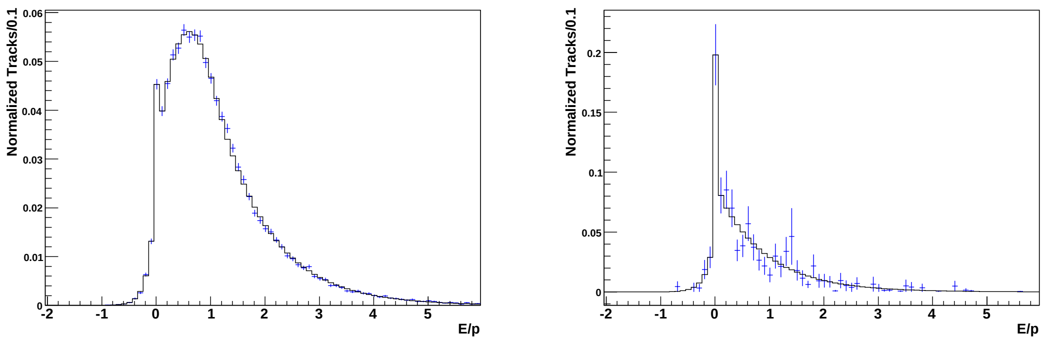

(a) E/p^{meas} (b) E/p^{bg}

Figure 7: The measured and background E/p distributions used for extracting the E/p of isolated pions at 1GeV. Statistical fluctuations were smoothed with a fit before solving the system via matrix inversion. Error bars show the statistical error on the unsmoothed distribution.

The mean of E/p^{iso} can be found more accurately without deconvoluting the background but by subtracting the average of the distributions:

$$<E/p>^{iso} = <E/p>^{meas} - <E/p>^{contam}$$

This was used to examine the extent of biases caused by any remaining contamination or from the method itself. Results are shown is Table 5. The E/p values are consistent, without bias, to the single particle mean and indicate the method could be effective in measuring the E/p for $\pi^{\pm}$ in minimum bias. However, larger statistics are required to properly assess the precision of this method.

$\pi^{\pm}$ p_T	**minimum bias**	**single particle - after cuts**	**single particle - before cuts**
1 GeV	0.429 ± 0.052	0.449 ± 0.003	0.455 ± 0.002
2 GeV	0.622 ± 0.043	0.609 ± 0.003	0.611 ± 0.002
5 GeV	0.818 ± 0.015	0.786 ± 0.002	0.786 ± 0.002
10 GeV	0.870 ± 0.036	0.869 ± 0.001	0.868 ± 0.001

Table 5: $<E/p>$ obtained for $\pi^{\pm}$s at $p_T = 1, 2, 5, 10 GeV$ compared to $\pi^{\pm}$s in single particle events.

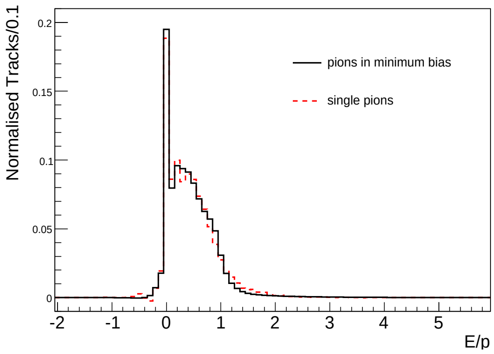

(a) p_T=1GeV

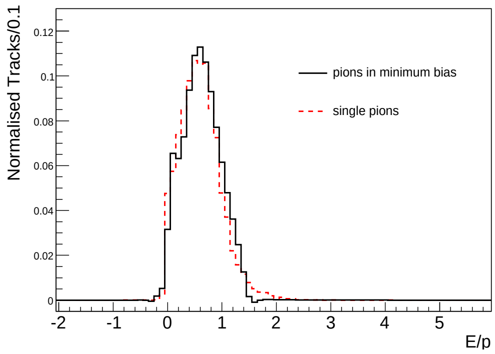

(b) p_T=2GeV

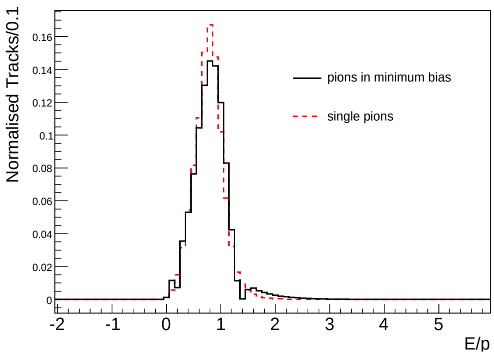

(c) p_T=5GeV

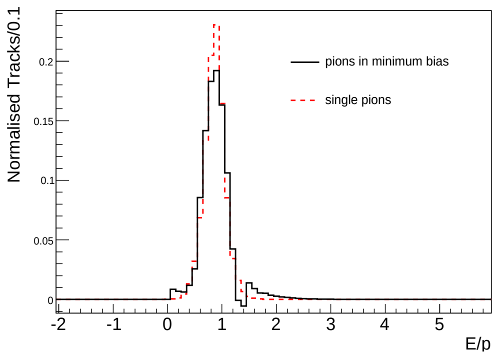

(d) p_T=10GeV

Figure 8: E/p obtained from deconvolution. For comparison, the energy distribution of “fake” clusters due to electronic noise in EM_{outer_cone} has been unfolded from the single $\pi^{\pm}$ E/p distributions.

7 Bias from non-pion tracks

Minimum bias events produce many charged particles with associated tracks. The majority are pions with a smaller number of kaons and protons. Less than 2% of tracks are due to heavier hadron, electrons, muons and fake tracks with no associated truth particle.

Table 6 lists the proportion of pions, kaons and protons in minimum bias based on information in the TrackTruthCollection after applying the cuts described in Section 6.1. 5,000 single kaons and protons were fully simulated using Athena 12.0.6.5 to assess the potential shift in the $< E/p >$ due to these fractions. The shift, assuming no other biases, to the pion E/p due to the presence of another particle types is given by $(< E/p >_{non_pion} - < E/p >_{pion}) * non_pion_tracks/all_tracks$. The results indicate this shift is 0.01 or below in all cases (see Table 6).

		1GeV	2GeV	5GeV	10GeV
Pions	Fraction (all)	75%	66%	64 %	62%
	Fraction (late showering)	75%	61%	65%	64%
	$< E/p >$	0.429 ± 0.052	0.622 ± 0.043	0.818 ± 0.015	0.870 ± 0.036
Kaons	Fraction (all)	15%	19%	23 %	27%
	Fraction (late showering)	22%	31%	27 %	32%
	$< E/p >$	0.511 ± 0.010	0.665 ± 0.008	0.782 ± 0.004	0.851 ± 0.004
	Potential shift	$+0.008 \pm 0.002$	$+0.010 \pm 0.002$	0.000 ± 0.001	$+0.004 \pm 0.001$
Protons	Fraction (all)	10%	14%	12%	09%
	Fraction (late showering)	03%	6%	07%	04%
	$< E/p >$	0.469 ± 0.017	0.571 ± 0.010	0.713 ± 0.006	0.818 ± 0.009
	Potential shift	$+0.001 \pm 0.002$	-0.006 ± 0.001	-0.008 ± 0.001	-0.004 ± 0.001

Table 6: Proportion of particle types for tracks in minimum bias after cuts

Table 6 also shows that the mix of particle type is different for late showering particles. This could introduce a bias if the contaminating background depends on particle type. The mean E/p obtained in minimum bias from all track types compared to just $\pi^{\pm}$ tracks is shown in Table 7. and suggests this may introduce a bias as large as +0.05 for 1 GeV and 2 GeV $\pi^{\pm}$ and -0.02 for 5 GeV and 10 GeV $\pi^{\pm}$s. However, the statistical error would need to be reduced to confirm this and to determine if its origin is from a mix of particle species or from limitations in the the background removal procedure.

$\pi^{\pm}$ p_T	**minimum bias - all tracks**	**minimum bias - $\pi^{\pm}$s only**
1 GeV	0.476 ± 0.040	0.429 ± 0.052
2 GeV	0.678 ± 0.028	0.622 ± 0.043
5 GeV	0.799 ± 0.012	0.818 ± 0.015
10 GeV	0.849 ± 0.029	0.870 ± 0.036

Table 7: ¡E/p¿ obtained from the background removal method for all tracks in minimum bias and for only $\pi^{\pm}$ tracks

8 Addition of pile-up

9 Conclusion and prospects

The minimum bias monte carlo used in this study represents only an order of days of data taking at a luminosity of $10^{3}1$ and trigger rate of 10Hz. It was found that this was sufficient to check the single hadronic energy calibration to within a precision of ??? % for p_Ts of 1-10 GeV .

Here we found that a method based on cuts alone could not be used to reduce contamination from extra particles. This was because very few pions in minimum bias are isolated. A method to measure the background and deconvolute it from the observed E/p distribution was applied. The resulting E/p was consistent with the E/p of single pions. The statistical uncertainties on the mean obtained from this method ranged between 0.015 (5GeV) and 0.052 (1 GeV). Therefore the extent of bias remaining from background particles and from the method itself needs to be understood by increasing the statistics.

The summary of all biases studied is given in Table 8. It was seen that the uncertainly in the pion energy scale is dominated by the unmeasurable contaminating energy (in the core cone and hadronic calorimeter), and the effect of non-pion tracks when estimating the background.

track p_T	**bias from cuts**	**unmeasurable background**	$\pi^{\pm}$ **energy mistaken as background**	**protons and kaons**	**combined bias**
1 GeV	-0.006 ± 0.004	0.015 ± 0.004	-0.024 ± 0.002	0.047 ± 0.014	0.032 ± 0.015
2 GeV	-0.002 ± 0.004	0.026 ± 0.005	-0.005 ± 0.001	0.056 ± 0.025	0.075 ± 0.025
5 GeV	0.000 ± 0.003	0.010 ± 0.007	-0.007 ± 0.000	-0.019 ± 0.012	-0.016 ± 0.014
10 GeV	0.001 ± 0.001	0.029 ± 0.021	-0.004 ± 0.000	-0.021 ± 0.026	0.005 ± 0.033

Table 8: Summary of biases in the E/p measurement method employed

With the first year of data taking it will be possible to reduce the statistical uncertainty on the E/p. It may also be possible to reduce the bias in the background measurement by applied additional cuts to those presented here. The data collected in one year should allow the local hadronic calibration to be checked as a function of η and ϕ, and for hadron p_Ts above 10 GeV.

References

[1] , .

Appendices